

# RECENT RESULTS ON THE $p_T$ DEPENDENCE OF PION INTERFEROMETRY FROM NA44<sup>1</sup>

NA44 Collaboration

H. Beker<sup>3,a</sup>, H. Bøggild<sup>4</sup>, J. Boissevain<sup>5</sup>, M. Cherney<sup>6</sup>, J. Dodd<sup>7</sup>,  
S. Esumi<sup>8</sup>, C.W. Fabjan<sup>3</sup>, D.E. Fields<sup>9</sup>, A. Franz<sup>3</sup>, K.H. Hansen<sup>4</sup>,  
B. Holzer<sup>3</sup>, T. Humanic<sup>9,b</sup>, B. Jacak<sup>5</sup>, R. Jayanti<sup>2,9,b</sup>, H. Kalechofsky<sup>9</sup>,  
T. Kobayashi<sup>10,c</sup>, R. Kratadze<sup>3,d</sup>, Y.Y. Lee<sup>9</sup>, M. Lelchouk<sup>7</sup>, B. Lörstad<sup>11</sup>,  
N. Maeda<sup>8</sup>, A. Medvedev<sup>7</sup>, Y. Miake<sup>12,e</sup>, A. Miyabayashi<sup>11</sup>,  
E. Neteboom<sup>6</sup>, M. Murray<sup>12</sup>, S. Nagamiya<sup>7</sup>, S. Nishimura<sup>8</sup>,  
S.U. Pandey<sup>9</sup>, F. Piu<sup>3</sup>, V. Polychronakos<sup>13</sup>, M. Potekhin<sup>7</sup>, G. Poulard<sup>3</sup>,  
A. Sakaguchi<sup>8</sup>, M. Sarabura<sup>5</sup>, K. Shigaki<sup>3,f</sup>, J. Simon-Gillo<sup>5</sup>,  
W. Sondheim<sup>5</sup>, T. Sugitate<sup>8</sup>, J. P. Sullivan<sup>5</sup>, Y. Sumi<sup>8</sup>, H. van Hecke<sup>5</sup>,  
W.J. Willis<sup>7</sup>, and K. Wolf<sup>12</sup>

<sup>3</sup> CERN, CH-1211 Geneva 23, Switzerland.

<sup>4</sup> Niels Bohr Institute, DK-2100 Copenhagen, Denmark.

<sup>5</sup> Los Alamos National Laboratory, Los Alamos, NM 87545, USA.

<sup>6</sup> Creighton University, Omaha, NE, USA.

<sup>7</sup> Columbia University, New York, NY 10027, USA.

<sup>8</sup> Hiroshima University, Higashi-Hiroshima 724, Japan.

<sup>9</sup> University of Pittsburgh, Pittsburgh, PA 15260, USA.

<sup>10</sup> National Laboratory for High Energy Physics, Tsukuba 305, Japan.

<sup>11</sup> University of Lund, S-22362 Lund, Sweden.

<sup>12</sup> Texas A&M University, College Station, TX 77843, USA.

<sup>13</sup> Brookhaven National Laboratory, Upton, NY 11973, USA.

<sup>a</sup> Present address: Rome I Institute, Rome I-00185, Italy

<sup>b</sup> Now at Dept. of Physics, Ohio State University, Columbus, OH 43210, USA

<sup>c</sup> Now at Riken Linac Laboratory, Riken, Saitama 351-01, Japan.

<sup>d</sup> Visitor from Tbilisi State University, Tbilisi, Rep. of Georgia.

<sup>e</sup> Now at Tsukuba University, Tsukuba 305, Japan.

<sup>f</sup> University of Tokyo, Tokyo 113, Japan.

Received 23 December 1993, in final form 8 February 1994, accepted 10 February 1994

The  $p_T$  dependence of  $\pi^+ \pi^+$  correlations from S + Pb collisions at 200 GeV/c per nucleon is presented as measured by the focusing spectrometer of the NA44 experiment at CERN. Multi-dimensional fits are performed to characterize the pion emission volume.

<sup>1</sup> Presented by Rama Jayanti at School and Workshop on Heavy Ion Collisions, Bratislava, 13-18 September 1993

<sup>2</sup> E-mail address: RAMA%VDGVSD@MPS.OHIO-STATE.EDU

## 1. Introduction

Two-particle intensity interferometry can provide information on the space-time extent of a particle-emitting source when the emitted radiation is at least partially incoherent [1,2,3]. Correlation measurements with identified particles may be particularly helpful in understanding the dynamical evolution of heavy-ion collisions. It has been argued that such measurements may provide evidence for the existence of a first-order phase transition in such collisions.

NA44 is a second generation experiment optimized for the study of identified single- and two-particle distributions at mid-rapidity. The spectrometer ('Focusing momentum difference' is designed to have good acceptance of pairs of particles with small momentum difference at midrapidity. The apparatus also has excellent momentum resolution ( $\delta p/p \approx 0.2\%$ ) and allows the study of particle distributions over a wide  $pr$  range ( $0.0 \leq pr \leq 1.5$ ). Our statistics permit multi-dimensional fits which are more sensitive to interesting dynamics and variables which are not influenced by relativistic correlation functions [3]; however an exponential distribution could arise owing to particle-production dynamics such as string-breaking [6] or decay of resonances [7,8]. A good clear signal of freeze out could come from higher  $pr$  pions since they are expected to leave the system earlier in time and are less contaminated by resonance decays. The RQMD event generator [9] which simulates heavy ion collisions predict that, while for  $pr$  lower than 200 MeV/c about 34% of the pions come from resonance decays only about 10% of the high  $pr$  ( $pr \approx 500$  MeV/c) pions come from resonance decays [10].

## 2. Experimental Set-Up

The layout of the experiment is shown in Fig. 1. The focusing spectrometer of the NA44 experiment has been described in detail elsewhere [11]. Three dipole magnets (D1, D2, and D3) and three quadrupoles (Q1, Q2, and Q3) create a magnified image of the target in the spectrometer. Only one charge sign can be detected in the

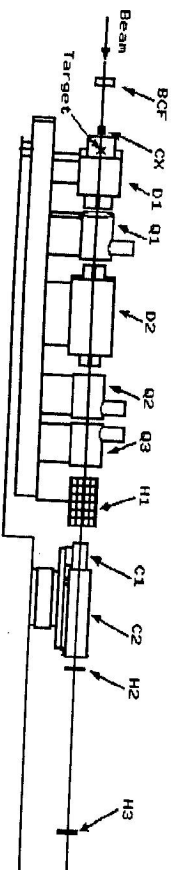


Fig. 1. The NA44 experimental set-up.

spectrometer at a time. The momentum range selected in this analysis covers a band of  $\pm 20\%$  at its nominal momentum setting of 4 GeV/c. The spectrometer is used in two settings, via 44 mrad and 122 mrad with respect to the beam axis to map

the rapidly  $pr$  space. The former one is referred to as the low  $pr$  (mean  $pr \approx 150$  MeV/c) while the latter one is referred to as high  $pr$  (mean  $pr \approx 450$  MeV/c) setting. The beam rate and time-of-flight start signal for sulphur beam are determined using a Cherenkov beam counter labelled CX seen in Fig. 1. The intrinsic time resolution of the Cherenkov beam counter is approximately 35 ps [12]. A silicon pad detector is used to measure the charged-particle multiplicity distribution with  $2\pi$  phi acceptance in the pseudorapidity range  $1.5 < \eta < 3.3$ .

The spectrometer uses three highly segmented scintillator hodoscopes, labeled H1, H2, and H3 [3] seen in Fig. 1, for tracking and time-of-flight measurements. In this analysis we use only the time measured on H3 for particle identification with a time resolution of approximately 100 ps. Time-of-flight along with the threshold cherenkov provide good particle identification. Four wire chambers are used for momentum calibration in conjunction with the third dipole magnet. A uranium-scintillator calorimeter (UCAL) allows identification of  $e$ ,  $\pi$ , and  $\mu$  and was not used in this analysis.

## 3. Data Analysis

Fits are performed in one and three dimensions. Fits in one dimension use  $Q = \sqrt{q^2 + q_0^2}$  which is good for comparison with other experiments and different particles, especially when one has limited statistics. Since the one dimensional fits are difficult to interpret one gets around it by fitting in three dimensions,  $Q_o$ , parallel to the momentum sum,  $Q_t$ , perpendicular to this and to the beam, and  $Q_l$ , parallel to the beam. Being parallel to the velocities of the particles,  $Q_o$  is sensitive to the lifetime of the source [7]. Data are analyzed in the frame in which the  $P_z$  sum of both particles is zero, coupling the lifetime information solely to  $Q_o$  [7]. This frame complicates the interpretation of  $Q_l$  which is anyway complicated by relativistic effects.

The spectrometer is used with two different settings, called horizontal and vertical, which optimizes our acceptance in  $Q_o$  and  $Q_t$ , respectively. In the horizontal setting for S + Pb collisions at 200 GeV/c per nucleon the data samples contains 40,000 reconstructed  $\pi^+$  pairs, while in the vertical setting we have 30,000  $\pi^+$  pairs.

The single-particle acceptance curve for both the horizontal and vertical settings are shown in Fig. 2, and span the rapidity range from 2.4 to 3.3, and a  $pr$  range from 0.20 to 1.3 GeV/c.

The target used in this analysis was 0.5cm thick. (i.e. 3% interaction length). There is no centrality (small impact parameter) requirement in this data sample. However, the spectrometer two-particle trigger bias the data towards the top 10% of the cross section determined by the silicon multiplicity detector.

Tracks are reconstructed from hit positions on the three hodoscopes, with pattern recognition constrained by straight-line trajectories after the magnets. The  $\chi^2$  of the fit in the vertical direction provides additional track-quality information. Cherenkov pulse and the mass-squared spectra give particle identification. Fig. 2. shows the distribution of the calculated mass-squared distributions (Contamination of  $\pi$  pairs by  $K$  is estimated to be less than 1%). A cluster algorithm based on hodoscope slat ADC pulse height distributions was used to distinguish pairs hitting neighboring slats on the hodoscopes from single tracks.

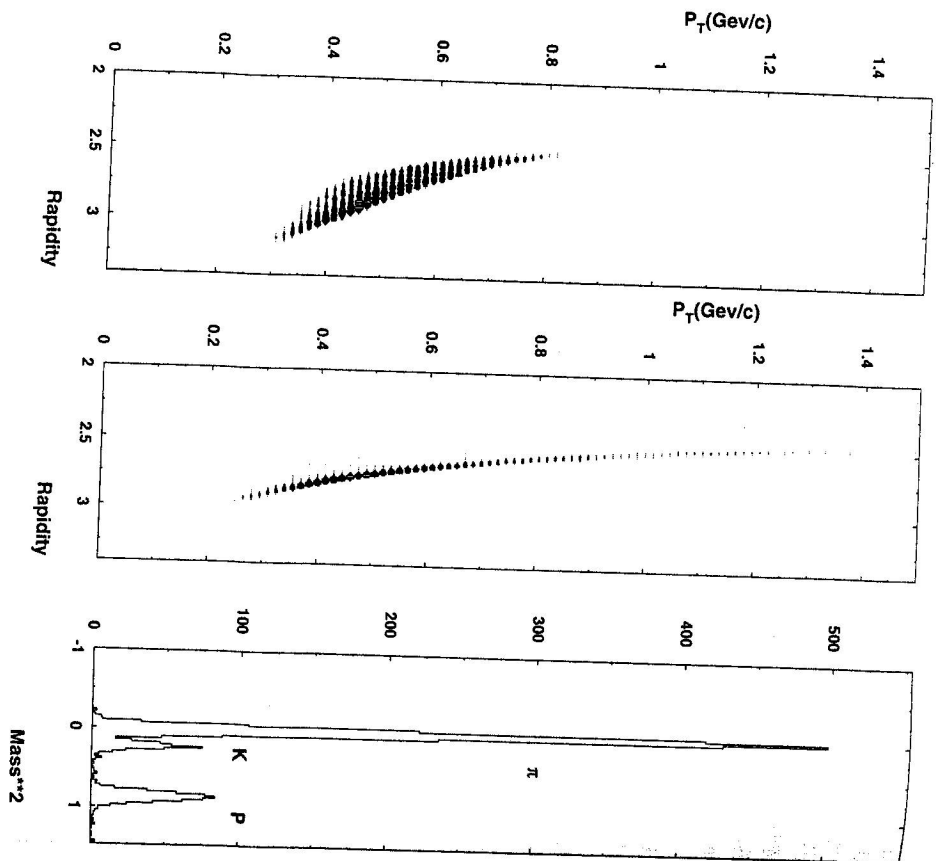


Fig. 2. The NA44 acceptance and mass squared plots.

The correlation function is determined using

$$C_{raw}(\vec{k}_1, \vec{k}_2) = \frac{R(\vec{k}_1, \vec{k}_2)}{B(\vec{k}_1, \vec{k}_2)}, \quad (1)$$

where  $\vec{k}_i$  are the particle momenta. The 'real distribution'  $R(\vec{k}_1, \vec{k}_2)$  is the distribution of the relative momentum, and the 'background distribution'  $B(\vec{k}_1, \vec{k}_2)$  is constructed from tracks mixed randomly from all events contained in  $R(\vec{k}_1, \vec{k}_2)$ . The background distribution is generated as follows: for each event in  $R(\vec{k}_1, \vec{k}_2)$ , twenty pairs of events are selected randomly to form the background pairs. In these pairs, one particle in

Recent results on the  $p_T$  dependence...

each event is selected randomly to create a new 'event' for the  $B(\vec{k}_1, \vec{k}_2)$  distribution. Thus the statistical error is dominated by the data sample. As in the real distribution, events from  $B(\vec{k}_1, \vec{k}_2)$  are rejected when the tracks share hits on the same slat of the hodoscopes. Tracks hitting neighboring slats in H1 are rejected as well, since most single particles hit two slats. Thus effects due to the loss of close-by pairs cancel for the two-particle correlation. This ensures that the 'real' and 'background' distributions are from the same class of collisions.

The background spectrum is distorted compared to the ideal uncorrelated two-particle spectrum owing to the effect of the two-particle correlations on the single-particle spectrum and is iteratively corrected for in the data ( $K_{SPC}$ ) [11,14,15]. When an iterative procedure is applied for the background correction, one finds the results to converge in about four iterations. The data are further corrected for the distortion of the two-particle spectrum by the momentum resolution of the spectrometer and the two-particle acceptance of the detectors ( $K_{acc}$ ).

Furthermore, two-particle correlations arising from coulomb interactions are corrected by the standard Gamow correction ( $K_{coul}$ ). Corrections based on the more accurate Coulomb wave function integration method tend to increase the extracted radius parameter by about 5% but do not affect the chaoticity parameter defined in Eq. (3) significantly. Coulomb interactions with the residual nuclear system are neglected but should be less important for two particles with identical charge-to-mass ratios which experience similar accelerations in the Coulomb field [16]

$$C(k_1, k_2) = C_{raw} \cdot K_{SPC} \cdot K_{acc} \cdot K_{coul} \quad (2)$$

Final state strong interactions arising due to particles of opposite charge in a high-particle-density environment are not corrected for owing to the large uncertainties in proposed procedures, no corrections are applied for them [16]. Hence the correlation function after all corrections applied is given by Eq. (2).

The data are fit with two different functions:

$$C(Q, Q_0) = A(1 + \lambda e^{-(Q + Q_0)^2 R^2}), R = \tau \quad (3)$$

or

$$C(Q_o, Q_i, Q_l) = A[1 + \lambda \exp(-Q_o^2 R_o^2 - Q_i^2 R_i^2 - Q_l^2 R_l^2)]. \quad (4)$$

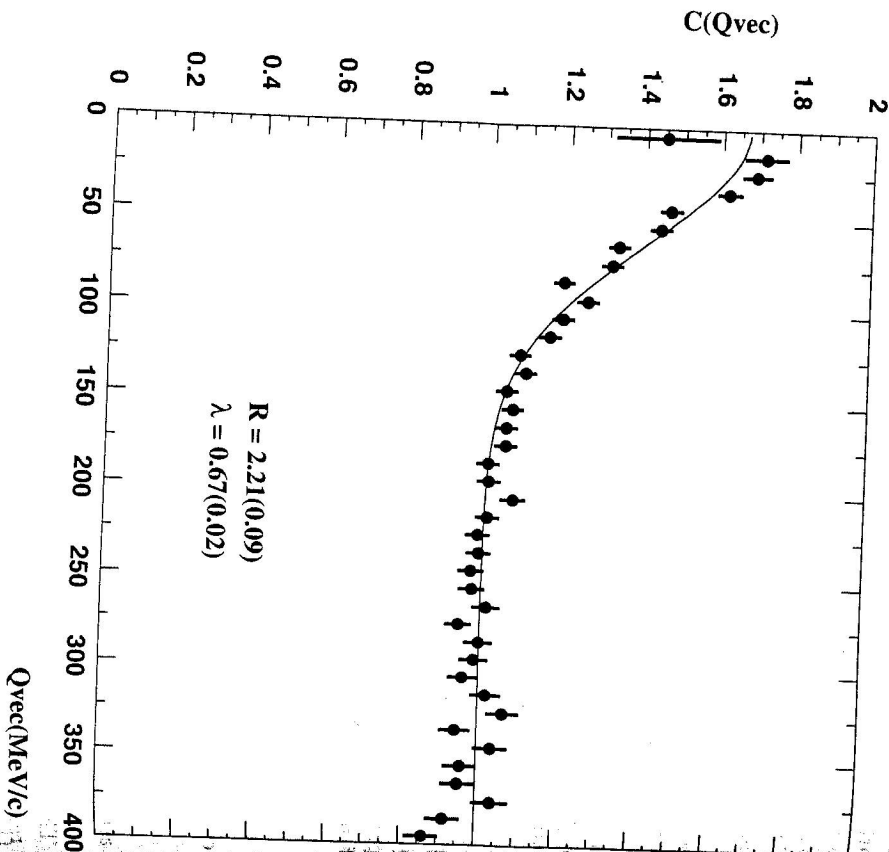
Fits are performed using maximum likelihood techniques assuming Poisson fluctuations. Fitting the three-dimensional equation requires using data from two different spectrometer settings, horizontal and vertical, and the data sets are fit simultaneously. The resolution in  $Q_o, Q_i$  and  $Q_l$  in the horizontal setting is about 15 MeV/c and the resolution in  $Q_o$  in the vertical setting is about 30 MeV/c. Bin sizes of 10 MeV/c have been employed in this data analysis.

#### 4. Results

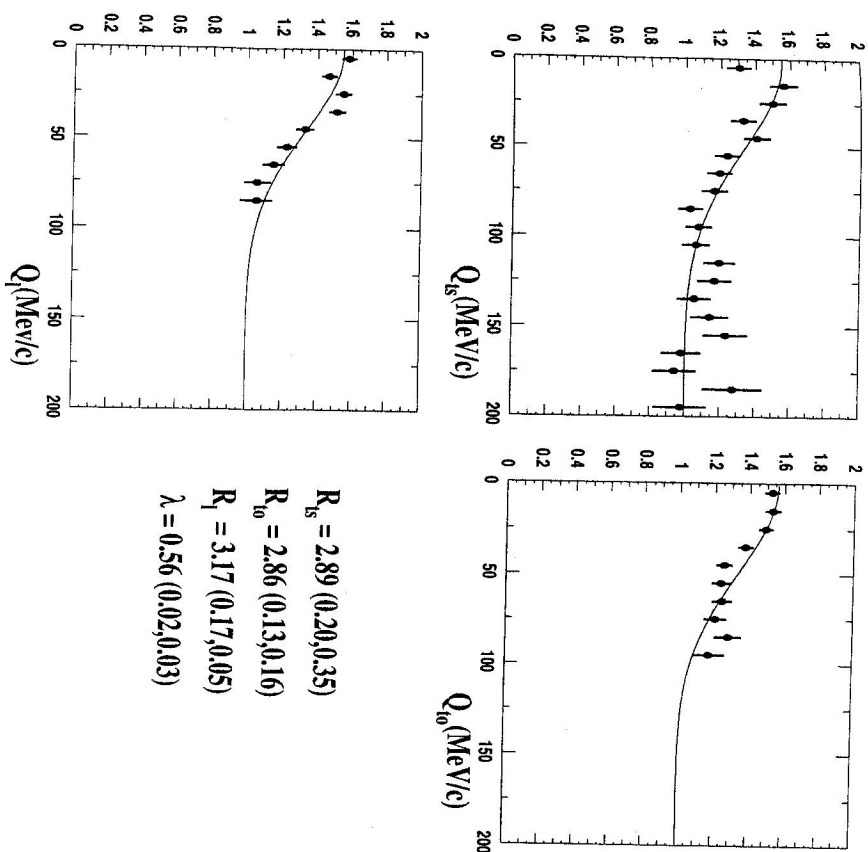
The results for the fit to  $Q$  ( $R = \tau$ ) for the horizontal spectrometer setting are summarized in Table 1 and shown together with the data in Fig. 3. The source parameters extracted from  $Q$  are difficult to interpret physically although useful to compare different data sets.

Table 1. Fitted results of Gaussian parametrizations in  $Q$ ,  $R = \tau$  (Preliminary)

System	$\lambda$	$R$ (fm)	$\chi^2/N_{dof}$
High- $p_T$ $\pi^+ \pi^+$	$0.67 \pm 0.02$	$2.21 \pm 0.09$	62/37
Low- $p_T$ $\pi^+ \pi^+$	$0.71 \pm 0.02$	$1.02 \pm 0.10$	58/36
Low- $p_T$ $k^+ k^+$	$0.88 \pm 0.06$	$2.78 \pm 0.26$	67/40

Fig. 3. The  $Q$  plots from the horizontal setting. The line represents a gaussian fit to data points (Preliminary).

Three-dimensional fits are performed on the  $S+Pb$   $\pi^+$  data set and results are shown in Table 2. Projections onto the three axes are presented in Fig. 4.

Fig. 4. The  $Q_s$ ,  $Q_{ls}$  and  $Q_l$  projections. The line represents a gaussian fit to the data points (Preliminary).

One can see the trend in data. Going from low  $p_T$  to high  $p_T$  the radius parameter decreases in case of pions. The radii in case of low  $p_T$  kaon [17] and high  $p_T$  pions are comparable.

## 5. Discussion

The pion radius extracted here is smaller than the pion radius extracted from lower  $p_T$  data set [18]. This could be due to a smaller resonance background and/or

Table 2. Fitted results of Gaussian parametrizations in  $Q_o$ ,  $Q_t$ , and  $Q_l$  (Preliminary)

System	$\lambda^{Gauss}$	$R_{o_o}^{Gauss}$ (fm)	$R_{t_s}^{Gauss}$ (fm)	$R_{l_s}^{Gauss}$ (fm)	$\chi^2/N_{dof}$
High- $pr$ $\pi^+ \pi^+$	$0.56 \pm 0.02$	$2.86 \pm 0.13$	$2.89 \pm 0.20$	$3.17 \pm 0.17$	16979/5834
Low- $pr$ $\pi^+ \pi^+$	$0.55 \pm 0.02$	$4.08 \pm 0.13$	$4.35 \pm 0.24$	$4.90 \pm 0.25$	14268/5863
Low- $pr$ $K^+ K^+$	$0.76 \pm 0.06$	$2.67 \pm 0.17$	$2.43 \pm 0.26$	$2.82 \pm 0.27$	25068/1980

reflect that high  $pr$  pions decoupling from the source at a earlier time than low  $pr$  pions. As mentioned earlier this is consistent with the RQMD prediction of decrease in resonance contribution as one goes to higher  $pr$ . Resonances influence the  $R_T$  distributions and have important effects on correlation functions, especially pions. A resonance important for the shape of the correlation is  $\omega$ , the effect of which decreases considerably going from low  $pr$  to high  $pr$  [19].

### Acknowledgements

The NA44 Collaboration wishes to thank the staff of the CERN PS-SPS accelerator complex for their excellent work. We thank the technical staff at CERN and the collaborating institutes for their valuable contribution. We are also grateful for the support given by the Science Research Council of Denmark; the Japanese Society for the Promotion of Science, and the Ministry of Education, Science and Culture, Japan; the Science Research Council of Sweden; the US Department of Energy; and the National Science Foundation (Nuclear Physics) through grants PHY8906284 and PHY8958491.

### References

- [1] R. Hanbury-Brown, R.Q. Twiss: *Nature* **178** (1956), 1046
- [2] M. Gyulassy, S.K. Kauffmann, L.W. Wilson: *Phys. Rev. C* **20** (1979), 2267
- [3] B. Lorstad: *Int. J. Mod. Phys. A* **4** (1988), 2861
- [4] S. Pratt: *Phys. Rev. D* **33** (1986), 1314
- [5] G. Bertsch, G.E. Brown: *Phys. Rev. C* **40** (1989), 1830
- [6] B. Andersson, W. Hofmann: *Phys. Lett. B* **169** (1986), 364
- [7] S. Pratt, T. Csörgő, J. Zimanyi: *Phys. Rev. C* **42** (1990), 2646
- [8] R. Lednicky, T.B. Progulova: *Z.Phys. C* **55** (1992), 295
- [9] H. Sorge, H. Stöcker, W. Greiner: *Nucl. Phys. A* **498** (1989), 567c
- [10] J. Sullivan et al.: *Phys. Rev. Lett.* **70** (1992),
- [11] H. Boggild et al.: *Phys. Lett. B* **302** (1993), 510
- [12] N. Maeda et al.: *A gaseous beam-counter with time resolution of 24 ps for relativistic nuclear beams*, to be published
- [13] T. Kobayashi, T. Sugitate: *Nucl. Instr. Meth. A* **287** (1990), 389

- [14] K. Kadja, P. Seyboth: *Phys. Lett. B* **287** (1992), 362
- [15] W.A. Zajc et al.: *Phys. Rev. C* **29** (1984), 2173
- [16] D. Boal, C. Gelbke, B. Jennings: *Rev. Mod. Phys.* **62** (1990), 553
- [17] H. Boggild et al.: *Identified kaon interferometry at CERN SPS*, to be published
- [18] H. Boggild et al.: *Directional analysis of identified pion interferometry at CERN SPS*, to be published
- [19] *Proc. 10th. Int. Conference on Ultrarelativistic Nucleus-Nucleus Collisions; Quark Matter 1993*, Nucl. Phys. A **544** (1994), 1;